Healthy aging and muscle function are positively associated with NAD(+) abundance in humans

ARTICLES
https://doi.org/10.1038/s43587-022-00174-3

nature aging

Healthy aging and muscle function are positively associated with NAD$^+$ abundance in humans

Georges E. Janssens[1,7], Lotte Grevendonk[2,3,7], Ruben Zapata Perez[1], Bauke V. Schomakers[1,4], Johan de Vogel-van den Bosch[5], Jan M. W. Geurts[6], Michel van Weeghel[1,4], Patrick Schrauwen[2,3], Riekelt H. Houtkooper[1] ✉ and Joris Hoeks[2,3] ✉

Skeletal muscle is greatly affected by aging, resulting in a loss of metabolic and physical function. However, the underlying molecular processes and how (lack of) physical activity is involved in age-related metabolic decline in muscle function in humans is largely unknown. Here, we compared, in a cross-sectional study, the muscle metabolome from young to older adults, whereby the older adults were exercise trained, had normal physical activity levels or were physically impaired. Nicotinamide adenine dinucleotide (NAD$^+$) was one of the most prominent metabolites that was lower in older adults, in line with preclinical models. This lower level was even more pronounced in impaired older individuals, and conversely, exercise-trained older individuals had NAD$^+$ levels that were more similar to those found in younger individuals. NAD$^+$ abundance positively correlated with average number of steps per day and mitochondrial and muscle functioning. Our work suggests that a clear association exists between NAD$^+$ and health status in human aging.

Over the past few decades, remarkable achievements in healthcare have led to a dramatic increase in the average life expectancy in most economically developed countries[1,2]. However, this increased life span is not paralleled by an increase in health span, as aging is accompanied by the development of various age-related pathologies, including metabolic disorders[3]. Understanding and targeting the aging process itself, rather than treating the symptoms of these age-related pathologies, may be the most effective strategy to prevent or counteract aging-related health decline[4].

The development of many age-related diseases has been associated with disturbances in mitochondrial metabolism, a hallmark of the aging process[5]. In that context, we and others have previously shown in both muscle and liver that pathways involved in oxidative phosphorylation (OXPHOS), fatty acid oxidation and mitochondrial biogenesis are impaired in aged mice[6,7]. In addition, we also reported that aged *Caenorhabditis elegans* are characterized by a prominent accumulation of most fatty acid species, which appeared to be controlled, at least in part, by the mitochondrial metabolic regulator AMPK[8]. Together, these preclinical studies highlight that alterations in various metabolic pathways, particularly within mitochondrial metabolism, are linked to the aging process and could therefore explain age-related metabolic complications.

Skeletal muscle is highly affected by the aging process[9], and age-induced loss of skeletal muscle mass and function have been related to mobility impairments[10,11], an increased risk of falls[12,13] and physical frailty[14]. Aging is also associated with a decline in muscle metabolism, as exemplified by a decrease in insulin sensitivity, metabolic inflexibility, increased oxidative damage and the occurrence of skeletal muscle mitochondrial dysfunction[15–17]. On the other hand, regular exercise positively impacts muscle metabolism and function, and regular exercise training has been shown to protect against aging-induced deterioration of muscle health[18,19].

Based on these considerations, the aims of the present study were to investigate the muscle metabolome comparing young and aged individuals and identify whether differences in aged individuals are associated with muscle and mitochondrial function. This comparison was expanded upon by evaluating changes in three groups of older individuals recruited according to their 'muscle health' states; aged individuals who (1) were exercise trained ('trained' older adults), (2) possessed typical physical activity abilities ('normal' older adults) or (3) displayed an impaired physical function ('impaired' older adults). Our results show that NAD$^+$ was one of the most depleted metabolites with age and that age-related NAD$^+$ depletion followed a 'healthy aging' trend, whereby 'physically impaired' older individuals were marked by significantly lower NAD$^+$ levels and exercise-trained older individuals could maintain NAD$^+$ abundance to levels nearly as high as those found in younger individuals. Furthermore, we found that in the older adults, NAD$^+$ muscle abundance positively correlated with muscle and mitochondrial health parameters. Taken together, these results show that NAD$^+$ is lower in aging human muscle and that NAD$^+$ abundance is directly associated with the healthy aging state of the individual.

Results

The metabolome of human muscle aging. In order to better understand which metabolites were associated with aging and establish a healthy aging muscle signature, we turned to an extensively characterized cohort of young and aged individuals, which we previously established (clinicaltrials.gov identifier NCT03666013).

[1]Laboratory Genetic Metabolic Diseases, Amsterdam UMC, University of Amsterdam, Amsterdam Gastroenterology, Endocrinology, and Metabolism, Amsterdam Cardiovascular Sciences, Amsterdam, The Netherlands. [2]Department of Nutrition and Movement Sciences, NUTRIM School of Nutrition and Translational Research in Metabolism, Maastricht University, Maastricht, the Netherlands. [3]TI Food and Nutrition, Wageningen, the Netherlands. [4]Core Facility Metabolomics, Amsterdam UMC, University of Amsterdam, Amsterdam, the Netherlands. [5]Danone Nutricia Research, Utrecht, the Netherlands. [6]FrieslandCampina, Amersfoort, the Netherlands. [7]These authors contributed equally: Georges E. Janssens, Lotte Grevendonk.
✉e-mail: r.h.houtkooper@amsterdamumc.nl; j.hoeks@maastrichtuniversity.nl

a

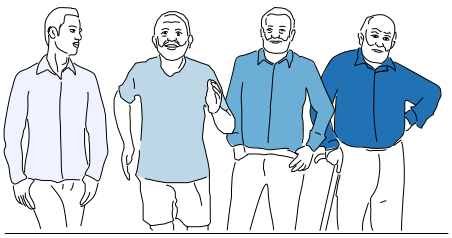

	Young	Older adults		
		Trained	Normal	Impaired
Participants	12	17	17	6
Age range (yr)	20–30	65–80	65–80	65–80
Male (%)	58	65	53	50
BMI (kg m^{-2})	22.7	23.9	25.8	27
Steps per day	10,153	13,671	10,197	6,608
Time high activity (%)	2.5	5.2	2.2	1.0

b

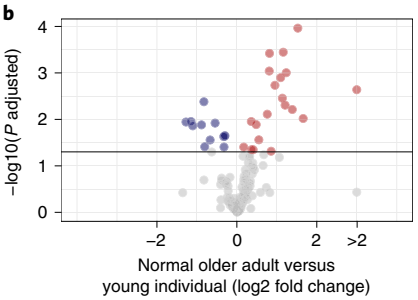

c

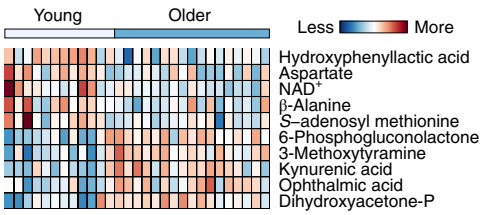

Fig. 1 | The metabolome of human muscle aging. a, Study participants consisted of either young or older adults; older adults were segmented into three categories: exercise trained, normally physically active or physically impaired with respect to their muscle health (Supplementary Table 1). Group averages are presented for body mass index (BMI), steps per day and high-intensity physical active time. **b**, Volcano plot of fold change (*x* axis, $\log_2$ scale) versus *P* value (*y* axis, −log10 scale) for older adults compared to young individuals with equal physical activity levels (young vs. normal older adults), illustrating significantly depleted (blue) or accumulated (red) metabolites with age (comparing young ($n=12$) and normal older adults ($n=17$)). The horizontal line indicates significance ($p<0.05$). Significance was determined using an empirical Bayes moderated *t* test (two sided, *P* values adjusted for multiple comparisons between groups)**. c**, Top five accumulating and depleted metabolites in normal older adults compared to young adults, depicted as a heatmap with higher (red) or lower (blue) relative abundance of metabolites. Source data: Statistical_Source_Data.csv.

This mixed-gender cohort consisted of individuals who were either young ($n=12$) or belonged to one of three age groups: trained older adults ($n=17$), older adults with normal physical activity levels ($n=17$) or physically impaired older adults ($n=6$). Participants were categorized into different study groups based on age, levels of self-reported physical exercise training and levels of physical function. Participants were considered normally physically active if they completed no more than one structured exercise session per week. Older participants were considered exercise trained if they engaged in at least three structured exercise sessions of at least 1 h each per week for an uninterrupted period of at least 1 yr prior to inclusion. Older participants were classified as physically impaired in case of a Short Physical Performance Battery (SPPB) score of ≤9 (Supplementary Table 1). Upon inclusion, further details on habitual physical activity levels were obtained using accelerometry. Over the course of 5 days, young individuals took an average of ~10,000 steps per day and spent 2.5% of their active time in high-intensity activities (Fig. 1a). The group of normal older adults was similar (~10,000 steps/day and 2.2% active time in high-intensity activities), ensuring that changes observed between these groups were age related rather than fitness related. Meanwhile, trained older adults were more active (~13,000 steps/day on average) with more time spent in high-intensity activities (5.2%), whereas the physically impaired older adults had a lower average daily step count (~6,000) and a lower amount of active time spent in high-intensity activities (1.0%) (Fig. 1a).

Using the muscle biopsy specimens collected from each participant in these groups, we performed ultrahigh-performance liquid chromatography coupled to high-resolution mass spectrometry-based metabolomics (Statistical Source Data). The results were used to establish a baseline understanding of the differences occurring between young and older adults with normal and equivalent levels of physical activity, taking into account all 137 metabolites we were able to annotate. Comparing the muscle metabolomes of these two groups using a principal-component analysis, we found a general separation between the groups to exist within the first two principal components, suggesting that aging imparts large changes in the muscle metabolome (Extended Data Fig. 1a).

To better understand what metabolites were contributing to the differences occurring with aging, we compared the accumulated and depleted metabolites (Fig. 1b and Extended Data Fig. 1b). We found a clear signature of changes to occur with normal aging (Fig. 1b). Intriguingly, when considering the top five metabolites either accumulating or depleting in older versus young adults with normal and equal physical activity, we found older adults to possess higher levels of ophthalmic acid, an oxidative stress marker[20,21], and dihydroxyacetone-phosphate and 3-methoxytyramine, two metabolite families negatively associated to mitochondrial respiration[22,23]. Moreover, we found that a significant age-related decline in NAD^+ occurs with aging. Together, these changes suggest an age-related change in oxidative metabolism in skeletal muscle (Fig. 1c).

NAD^+ abundance is directly related to healthy aging muscle. Having established the metabolic changes occurring with aging in muscle, which pointed toward alterations in oxidative metabolism, we next asked which of these differences were not only linked to aging but also related to muscle health levels. To do so, we ranked metabolites based on the degree to which their abundance level followed a health trend with the four groups, from young adults to trained older adults to normally active older adults to physically impaired older adults. This approach was designed to highlight metabolites that may be lower with normal aging, with a decline that is either (nearly) absent with regular exercise training or exacerbated by belonging to a physically impaired aging group. Plotting these correlations against the typical aging changes served to highlight the age-related changes that are important also on a health and exercise related axis. Remarkably, we found that changes in normal older adults and changes that follow a 'health trend' are highly correlated, implying that most metabolic changes that occur with age in the muscle can be reversed with regular exercise training (Fig. 2a).

In line with this observation, we found that NAD^+ not only was one of the most depleted molecules in older adults when compared

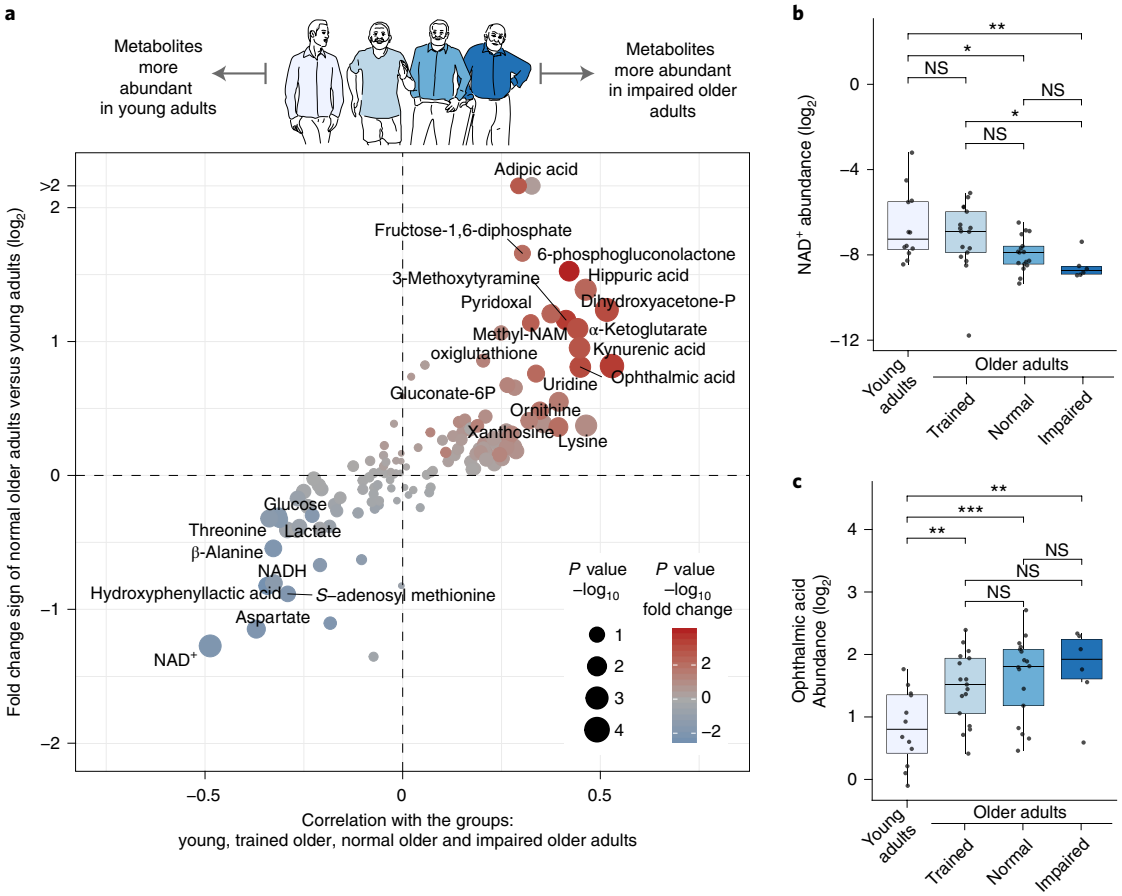

Fig. 2 | Muscle NAD⁺ levels are related to muscle health during aging. a, Comparison of the correlation a metabolite has to the four muscle health groups (young adults, trained older adults, older adults with normal physical activity levels and physically impaired older adults) (*x* axis), where the size of point on the graph indicates *P* value of the correlation ($-\log_{10}$ scale) and correlation and significance were determined using Pearson's product-moment correlation coefficient, and the fold change the metabolite undergoes in older versus young adults with normal physical activity (y axis), where the color of the point indicates the *P* value of aging fold change (with directionality represented as either increasing (red) or decreasing (blue)) and significance was determined using an empirical Bayes moderated *t* test (two sided, *P* values adjusted for multiple comparisons between groups). The metabolite's name is depicted when the aging fold change had a significance of $P < 0.05$. The graph reveals NAD⁺ to be depleted in aging and follow the strongest correlation to a healthy aging trend. **b**, Abundance levels of NAD⁺ in the four muscle health groups. **c**, Abundance levels of ophthalmic acid in the four muscle health groups. Sample sizes are $n = 12$ for young individuals, $n = 17$ for trained older adults, $n = 17$ for normal older adults and $n = 6$ for impaired older adults. Significance was determined using an empirical Bayes moderated *t* test (two sided, *P* values adjusted for multiple comparisons between groups: $^{*}P < 0.05$, $^{**}P < 0.01$, $^{***}P < 0.001$). In boxplots, the inner line within the box is the median of the data, the box extends to the upper and lower quartile of the dataset (25% of the data above and below the median), whiskers (dashed lines) represent up to 1.5 times the upper or lower quartiles and circles beyond the whisker represent individual data points outside this range. Source data: Statistical_Source_Data.csv (all exact *P* values for comparison between groups are listed therein).

to young individuals (Fig. 1c) but also displayed the strongest association with healthy aging (Fig. 2a). Indeed, age-related NAD⁺ differences (Fig. 1b) were exacerbated in impaired older adults (Fig. 2b and Extended Data Fig. 2a). Furthermore, according to Venn diagram analysis, significant age-related lower NAD⁺ levels were found to be in common only between the normal aging and impaired aging groups (Extended Data Fig. 2b). Meanwhile, the trained older adults group possessed levels of NAD⁺ comparable to those found in young adults (Fig. 2b and Extended Data Fig. 2b).

Interestingly, we found that ophthalmic acid, a marker of oxidative stress and one of the top five accumulated metabolites (Fig. 1c), displayed a trend opposite the one observed for NAD⁺; namely, a higher abundance was found in older adults compared to young adults, and this trend became exacerbated in physically impaired older adults but was attenuated in trained older adults (Fig. 2a,c). In addition, we found that oxiglutathione, another marker of oxidative stress, followed the same trend as ophthalmic acid (Fig. 2a), suggesting that NAD⁺ depletion with aging may occur in parallel with increased reactive oxygen species (ROS) production.

Modulation of the NAD⁺ pathway with aging. Our untargeted metabolomics data pointed toward oxidative metabolism as a central player in aging muscle. Having observed that NAD⁺ was both lower in normal aging and also possessed the strongest correlation with healthy aging, we next asked how the NAD⁺ pathway itself was modulated in older adults relative to young adults. To do so, we considered all metabolites related to NAD⁺ metabolism (Extended Data Fig. 3a–l) and mapped out how they changed in each group of older adults relative to young adults onto the NAD⁺ synthesis pathway (Fig. 3). The depletion of NAD⁺ in each group was mirrored by a depletion of NADH, although to a lesser extent (Fig. 3), and the ratio of NAD⁺ to NADH appeared to be maintained across all groups in general (Extended Data Fig. 4a). Furthermore, we observed a lack of modulation of NADP⁺ and NADPH in the older age groups,

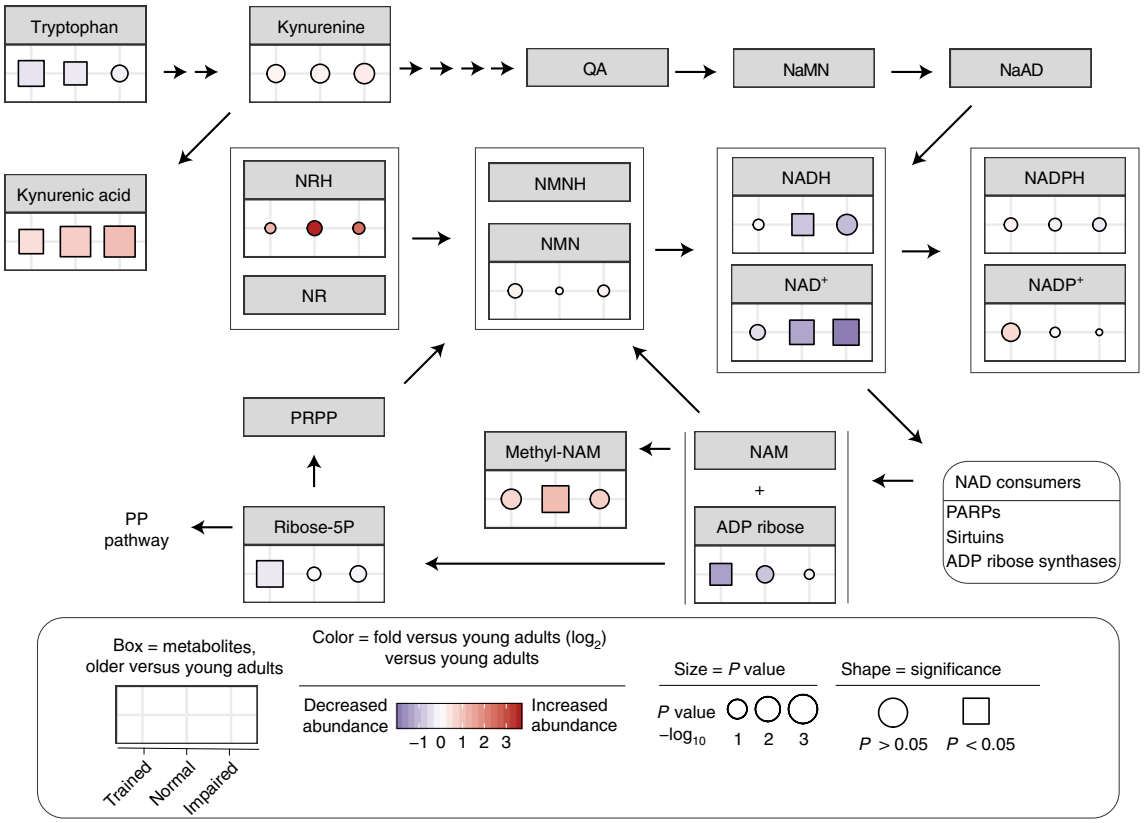

Fig. 3 | Major NAD⁺ metabolites and changes in healthy muscle aging. Changes in the three groups of older adults (trained, normally active and physically impaired) relative to young adults are depicted for each NAD⁺-related metabolite in the map. The color indicates the fold change (blue, decreased; red, increased), the size indicates the *P* value of the significance ($-\log_{10}$ scale) and the shape denotes a significance threshold (square, $P < 0.05$). Significance was determined using an empirical Bayes moderated t test (two sided, *P* values adjusted for multiple comparisons between groups). Source data: Statistical_Source_Data.csv, all exact *P* values for comparison between groups are listed therein. NaAD, nicotinic acid adenine dinucleotide; NaMN, nicotinic acid mononucleotide; NMN, nicotinamide mononucleotide; NMNH, nicotinamide mononucleotide (reduced); NR, nicotinamide riboside; NRH, nicotinamide riboside (reduced) ; PARP, poly ADP-ribose polymerase; PP, pyrophosphate; PRPP, phosphoribosyl pyrophosphate; QA, quinolinic acid.

which points to an aging- and exercise-dependent modulation of NAD(H), but not their phosphorylated forms.

Having established the association of NAD(H) with healthy aging, we next turned our attention to other metabolites involved in NAD⁺ de novo synthesis and recycling. We found a strong correlation between kynurenic acid accumulation and the healthy aging trend (Fig. 3 and Extended Data Fig. 3b). Kynurenic acid is produced by kynurenine aminotransferase-mediated irreversible transamination of kynurenine, a downstream metabolite of tryptophan in the NAD⁺ de novo synthesis pathway, or through ROS-mediated oxidative degradation of kynurenine[24]. This latter explanation is in line with our previously noted increase in the oxidative damage markers ophthalmic acid and oxiglutathione[20,21] in older adults (Fig. 2a,c), supporting the hypothesis that kynurenic acid is produced via ROS-mediated degradation of kynurenine.

To further explore the metabolomic responses involved in oxidative stress, we mapped out the glutathione and oxiglutathione pathways, which are generated by precursors such as glutamate and glycine (Extended Data Fig. 4b). Because electrons from glutathione are used to quench free radicals, forming oxiglutathione in the process, the glutathione/oxiglutatione ratio can be indicative of oxidative stress[20,21]. This type of stress occurs after a decrease in glutathione and/or an increase in oxiglutathione, ultimately producing a decrease in the glutathione/oxiglutathione ratio. As noted, ophthalmic acid is a marker for glutathione synthesis, reflecting oxidative stress[20,21]. In addition to the significant increase in ophthalmic acid previously noted (Fig. 2c), we found a significant increase in oxiglutathione for all aged groups relative to young subjects, resulting in a significant decrease in the glutathione/oxiglutathione ratio (Extended Data Fig. 4b). Although a trend was visible for lower oxiglutathione and thereby a higher glutathione / oxiglutathione ratio in athletic older adults relative to impaired older adults, these were not significant (Extended Data Fig. 4b). Although these reported ratios do not directly correspond to biological ratios of these metabolites, due to different ionization efficiencies in the mass spectrometer between glutathione and oxiglutathione, the observed changes in this analytical glutathione/oxiglutathione ratio between groups are still physiologically meaningful. We also found that glutamate and glycine levels were similar across groups (Extended Data Fig. 4b). Although cysteine levels could not be determined in these samples, our data suggest that glutathione demand is increased due to an increased oxidative milieu that occurs with aging and that this increased demand is possibly depleting cysteine stores.

NAD⁺ relates to mitochondrial function and muscle health. Our cohort possessed extensive phenotyping of muscle health parameters, which offered an unprecedented opportunity to better understand how the age-related decline in NAD⁺ related to various outcomes of muscle health, an unexplored domain in human physiology. To address this question, we performed a cross-correlation of the abundances of NAD⁺-related metabolites to muscle-related parameters previously measured (clinicaltrials.gov identifier NCT03666013) (ref. [25]) in the three groups of older adults (Extended Data Fig. 5a). Phenotypical parameters consisted of molecular

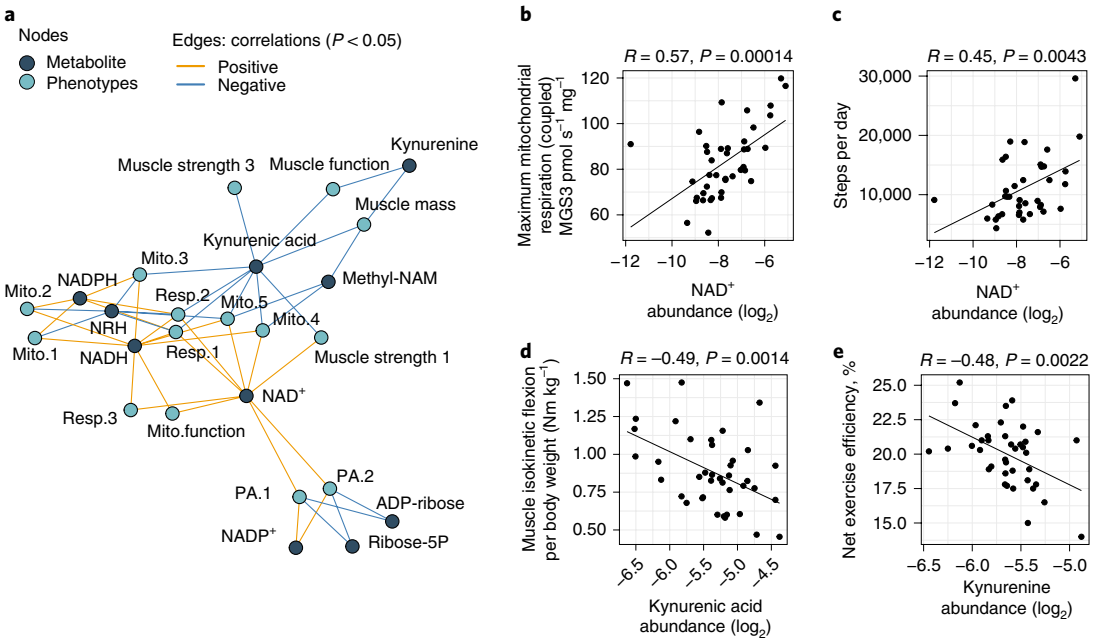

Fig. 4 | Molecular–physiological and NAD⁺-related healthy aging network. a, Network of significant associations between molecular–physiological parameters (light-blue nodes) and NAD⁺-related metabolites (dark-blue nodes). Positive associations are shown in orange, and negative associations are shown in blue; correlation and significance were determined in older adults using Pearson's product-moment correlation coefficient ($P < 0.05$). Sample consists of older adults ($n = 40$). Mito.1, Mitochondria - OXPHOS compl V blot (A.U.), Mito.2, Mitochondria - OXPHOS compl III blot (A.U.); Mito.3, Mitochondria - OXPHOS compl II blot (A.U.) Mito.4, Mitochondria - OXPHOS compl IV blot (A.U.), Mito.5, Mitochondria - OXPHOS compl I blot (A.U.); PA.1, Physical activity - steps per day; PA.2 Physical activity- % time high physical activity; Resp.1, Respiration - Coupled MOGS3 (pmol/(s*mg)); Resp.2, Respiration - Uncoupled MOGS (pmol/(s*mg)); Resp.3, Respiration - Coupled MGS3 (pmol/(s*mg)); Muscle strength 1, Muscle isokinetic extension / body weight (Nm/kg); Mito.function, Mitochondrial function - MRS PCr recovery rate. **b**–**e**, Scatterplots depicting selected correlations between metabolites and physiological parameters, highlighting the positive associations between NAD⁺ and mitochondrial respiration (**b**) ($R = 0.57$, $P = 0.00014$) and between NAD⁺ and average daily steps (**c**) and highlighting the negative associations between ($R = 0.45$, $P = 0.0043$) kynurenic acid and muscle strength (**d**) ($R = -0.49$, $P = 0.0014$) and kynurenine and exercise efficiency (**d**) ($R = -0.48$, $P = 0.0022$). Sample consists of older adults ($n = 40$), and P value represents significance of the Pearson's product-moment correlation coefficient. Source data (Statistical_Source_Data.csv) and physiological data are available in our previous study[25].

measurements of mitochondrial abundance (OXPHOS subunit abundances), mitochondrial respiration (oxygen consumption measurements in permeabilized muscle fibers) and in vivo mitochondrial function (Phosphocreatine (PCr) recovery), in addition to physiological parameters, including muscle energetics (net exercise efficiency percentage), muscle volume (magnetic resonance imaging), muscle strength (isokinetic function) and habitual physical activity (accelerometry) (Extended Data Fig. 5b). By comparing and focusing our analyses on the metabolite abundances that correlate or anti-correlate with these molecular and physiological parameters, we reasoned that a correlation network could map the landscape of NAD⁺-related interactions associated with healthy muscle aging.

This approach revealed that a network existed that strongly linked NAD⁺ metabolites to aging muscle function. Intriguingly, within this network, kynurenic acid acted as a hub of negative associations, whereas NAD⁺ was positively associated with many functional parameters of the muscle (Fig. 4a). For example, we found that NAD⁺ abundance had a strong positive association with maximum ADP-stimulated (state 3) mitochondrial respiration (Fig. 4b). Likewise, and quite remarkably, NAD⁺ abundance in muscle was also correlated with the average daily step count (Fig. 4c). Meanwhile, when considering negative correlations, we observed that kynurenic acid was inversely associated with isokinetic muscle strength (Fig. 4d), and kynurenine was inversely associated with net exercise efficiency (Fig. 4e). Taken together, this approach offered a view of the strong relationship between the NAD⁺ pathway and healthy aging muscle functioning in older individuals.

Numerous preclinical studies have indicated NAD⁺ depletion as the primary cause of disease and disability during aging[26]. Although we have seen that boosting NAD⁺ metabolism in humans induced only very minor physiological changes[27–29], increasing NAD⁺ in animal models improved, among other things, muscle recovery, endurance capacity, mitochondrial function, oxidative metabolism, insulin sensitivity and lipid profiles, and it extended life span[17,30–36]. In line with these preclinical studies, our NAD⁺-related metabolite and muscle physiology network supports that NAD⁺ abundance is indeed an indicator of muscle health status in aging individuals.

Discussion

In the current study, we investigated age-related muscle metabolomic changes by comparing young and aged individuals. We identified how metabolomic differences in aged individuals relate to muscle and mitochondrial function by evaluating changes across a healthy (muscle) aging trend. Out of the 137 detected metabolites, NAD⁺ was one of the most depleted metabolites upon aging, a finding that itself fills a void in the literature between preclinical animal research and clinical human research. Namely, to date, very few studies have established that NAD⁺, which declines in laboratory animals, also declines in human tissues[37]. Moreover, our study found not only that NAD⁺ levels are lower in aged adults compared to young adults but also that NAD⁺ levels are associated with the

health state of the aged individual. Specifically, NAD^+ is lowest in impaired older adults, whereas exercised-trained older adults show levels of NAD^+ similar to those of young individuals, and NAD^+ abundance was directly positively associated with mitochondrial respiration and physiological muscle functioning when considering all individual older adults.

In this study, the young and normal aging groups were not engaged in structured exercise activities, and both recorded approximately 10,000 steps daily. Although this is well above the general recommendations[38], our results suggest that maintaining a healthy physical activity level in older people that is comparable to younger people is not sufficient to prevent an age-related decline in NAD^+. However, endurance-trained older participants who had 12,500 steps per day and performed at least three exercise-training sessions per week did not show evidence of the lower NAD^+ levels that occur during normal aging. In contrast, physically impaired older adults in our study averaged less than 7,500 steps per day, reflecting a more sedentary lifestyle relative to the other participants[39]. The differences in habitual physical activity levels between the age groups were directly reflected in NAD^+ metabolism, whereby quite strikingly, daily step counts correlated strongly with muscle NAD^+ levels. Taken together, our results suggest that the best therapy to maintain youthful and physiologically important levels of NAD^+ during aging may simply involve highly structured exercise regimens, although this may not be realistic for all individuals.

Although an age-related decline in NAD^+ and the benefits of boosting NAD^+ levels have been extensively demonstrated in model organisms[17,30–36], relatively little evidence exists relating NAD^+ to aging and health in humans[37]. To our knowledge, to date, an age-related decline in NAD^+ levels in humans has only been demonstrated to occur in the brain (using magnetic resonance spectroscopy)[40,41] and pelvic skin samples (measured spectrophotometrically)[42]. Here, we further demonstrate that NAD^+ levels are lower with human aging in skeletal muscle. Interestingly, it has previously been shown in human skeletal muscle that levels of nicotinamide phosphoribosyltransferase (NAMPT), the rate-limiting enzyme in the NAD^+ salvage pathway, decreases with aging and that both aerobic and resistance exercise training can increase NAMPT levels[43]. Although the study was not designed to directly measure NAD^+, the findings are in line with ours, suggesting that a lifestyle with exercise is associated with higher NAD^+ levels compared to a lifestyle without intensive exercise in older adults.

Transcriptomic and metabolomic studies in human skeletal muscle have extensively been used in the context of frailty and sarcopenia, with key findings demonstrating changes in mitochondrial function, muscle growth and cell turnover[44–46]. One study demonstrated that NAD^+ (measured enzymatically) and mitochondrial oxidative capacity were decreased in sarcopenic older men relative to age-matched controls[47]. Although the study was not designed to investigate whether older adults had lower levels of NAD^+ than younger individuals in the first place, the findings are in line with ours and suggest that impaired older adults have lower NAD^+ levels than normal older adults. Taken together, our work complements these recent findings and incorporates both young and old individuals, possessing both athletic and impaired aging states, to solidify our understanding of NAD^+ in skeletal muscle healthy aging.

A number of open questions accompany our findings. First, we noted reduced ADP ribose in trained older adults relative to young adults despite comparable NAD^+ levels (Fig. 3 and Extended Data Fig. 3). This difference was not significant in normal and impaired older adults. Because ADP ribose is produced in part through the activity of NAD^+ consumers, a depletion of ADP ribose may suggest a reduction in the activity of NAD^+ consumers in trained older adults and therefore may indirectly result in higher levels of NAD^+. Results from other studies, however, point toward increased NAD^+ recycling via NAMPT upon exercise[43,48]. Because NAMPT requires phosphoribosyl pyrophosphate, which can be synthesized from ADP ribose by the activities of ADPrases[49,50] and the phosphoribosyl pyrophosphate synthase[51], the depletion in ADP ribose we observe may also fit the hypothesis that ADP ribose is used to produce NAD^+. More research is required to distinguish whether reduced consumption, or increased production, is the cause of the differences we observed in NAD^+ levels between the age groups. Second, we observed an increase in kynurenine and kynurenic acid with aging, which was negatively correlated with muscle function in our participants. Kynurenic acid accumulates with aging in human cerebrospinal fluid[52], underlies learning and memory impairment associated with aging in *C. elegans*[53] and has been implicated in many diseases associated with inflammation and aging ('inflammaging')[54–56]. Furthermore, it has recently been shown that trained muscle uses kynurenine metabolism to increase bioenergetic efficiency[57]. An open question emerges on how kynurenine may mechanistically relate to, rather than simply be associated with, the efficiency of muscle contraction in aging observed in our study. Third, our study focused on the NAD^+ pathway because of its prominent association with health in our data, but a number of other metabolites emerged from our analyses and deserve further investigation, including hydroxyphenyllactic acid, aspartate, β-alanine, and 3-methoxytyramine, among others, as these changed in a health-dependent manner with aging. It must therefore be noted that other factors are also at play, and not just NAD^+, in the relationship between muscle function and aging. Finally, several studies using NAD^+ precursors to boost NAD^+ levels did not find an association between NAD^+ levels and either skeletal muscle or mitochondrial functioning, suggesting that factors in addition to NAD^+ alone play a role in our observations[58,59].

Finally, several limitations should be considered in relation to our study. First, although the SPPB scores largely defined the placement of individuals in our different age and health groups, variations within the groups still exist. As a result, the group-based analyses (such as in Fig. 3) may have a lower resolution to detect differences than the ungrouped analyses (such as in Fig. 4). Second, the power calculation to determine the number of study participants was performed using the original primary outcome of the cohort studied (NCT03666013) (ref. [25]), which was the rate of ex vivo mitochondrial respiration. Therefore, the number of samples used in this study was based on this calculation and the sample availability at the time we performed metabolomics. Consequentially, several groups had low numbers of participants (such as in the impaired aging group), which may make subtler differences in the metabolome difficult to detect, and the low sample number makes it virtually impossible to meaningfully stratify the results across gender, body mass index and other demographic measures. Nonetheless, despite these low numbers and a diverse study population, we still found significant differences in the NAD^+ pathway, which serves to reinforce the fact that NAD^+ depletion in muscle is a profound phenotype of human aging. Third, our metabolomics were performed on muscle biopsies, which is an inherently heterogeneous sample type, both within and between individuals. This includes heterogeneity at the level of muscle fiber type (e.g., endurance-trained older individuals may have more type I rather than type II muscle fibers[60–62]) and intracellular heterogeneity (e.g., NAD^+ is present in both cytosolic and mitochondrial subcellular locations, which can be relevant for health[63]). Therefore, our study could not resolve whether the changes in NAD^+ abundance were due to ratio shifts in muscle fiber types or specific changes in subcellular NAD^+ pools. Further research is needed to resolve this issue. Finally, of fourth consideration, our work reports on a cross-sectional study population rather than a prospective study. Because of its cross-sectional design, our study does not prove that exercise can prevent the aging-related decline in muscle NAD^+ levels, and a follow-up prospective study is required to address this issue. Furthermore, our work does

not eliminate the possibility that if the physiology of an individual is such that they possess higher NAD^+ levels when they are older, then they may be predisposed to higher activity levels (reverse causation possibility). Therefore, causal involvement is difficult to conclude.

In summary, our study advances our understanding of the relevance of NAD^+ metabolism to human muscle aging, characterizing NAD^+ metabolism in extensively phenotyped young and older adults. Specifically, findings of our study include that (1) aging is associated with lower levels in skeletal muscle's NAD^+ abundance, occurring despite older adults maintaining adequate physical activity; (2) lower NAD^+ levels relate to impaired aging, and a high-intensity athletic aging lifestyle results in muscle NAD^+ levels similar to those seen in young adults; and (3) NAD^+ metabolism strongly correlates with human skeletal muscle health during aging, as assessed through mitochondrial and physical functioning, whereby the average daily step count of an older adult directly associates with their muscle NAD^+ levels. Together, this work affirms the relationship between NAD^+ levels and overall health status in aging individuals and highlights the NAD pathway as a promising target to promote healthy aging in humans.

Methods

Human subjects and procedures. Fifty-two participants, including 12 young (7 male and 5 female) and 40 older (23 male and 17 female) individuals, were recruited in the community of Maastricht and its surroundings through advertisements at Maastricht University, local newspapers, supermarkets and sports clubs. The study protocol was approved by the institutional medical ethical committee and conducted in agreement with the Declaration of Helsinki. All participants provided written informed consent, and the study was registered at clinicaltrials.gov with identifier NCT03666013. Participants received a fee to compensate for their time investment, along with compensation for travel expenses. Data collection and analysis were not performed blind to the conditions of the experiments. Physiological data from this cohort were reported in our previous study as part of a different analysis[25]. Fully annotated demographic data (e.g., sex and body mass index) for each individual participant is available as supplementary material therein. Before inclusion, all subjects underwent a medical screening that included a physical examination by a physician and an assessment of physical function using the SPP), composed of a standing balance test, a 4-m walk test and a chair-stand test. After the screening procedure, participants were categorized into to the following study groups: young individuals with normal physical activity (Y; 20–30 years), older adults with normal physical activity (NA; 65–80 years), athletic older adults (AA; 65–80 years) and physically impaired older adults (IA; 65–80 years). Participants were considered normal, physically active (NA) if they completed no more than one structured exercise session per week. Participants were considered trained (AA) if they engaged in at least three structured exercise sessions of at least 1 h each per week for an uninterrupted period of at least 1 yr Participants were classified as older adults with impaired physical function (IA) in case of an SPPB score of ≤9. The SPPB score was calculated according to the cutoff points determined previously[64]. Subject characteristics are summarized in Supplementary Table 1. A STROBE (STrengthening the Reporting of OBservational studies in Epidemiology) cross-sectional study checklist statement is available as supplementary information.

Muscle biopsy. At 9 AM, after an overnight fast from 10 PM the preceding evening, a muscle biopsy specimen was taken from the m. vastus lateralis under local anesthesia (1.0% lidocaine without epinephrine) according to the Bergström method[65]. Part of the biopsy specimen was immediately placed in an ice-cold preservation medium (BIOPS, OROBOROS Instruments) and used for the preparation of permeabilized muscle fibers and measurement of ex vivo mitochondrial oxidative capacity, as described earlier[66,67]. The remaining part of the muscle biopsy was immediately frozen in melting isopentane and stored at −−80 °C until further analysis.

Mitochondrial respiration. Permeabilized muscle fibers (~2.5 mg wet weight) were used for the assessment of mitochondrial capacity using a two-chamber oxygraph (OROBOROS Instruments), according to Hoeks et al.[68]. To prevent oxygen limitation, the oxygraph chambers were hyperoxygenated up to ~400 µmol l^{-1} O_2. Subsequently, two different multisubstrate/inhibition protocols were used in which substrates and inhibitors were added consecutively at saturating concentrations. State 2 respiration was measured after the addition of malate (4 mmol l^{-1}) plus octanoylcarnitine (50 µmol l^{-1}) or malate (4 mmol l^{-1}) plus glutamate (10 mmol l^{-1}). Subsequently, an excess of 2 mmol l^{-1} ADP was added to determine coupled (state 3) respiration. Coupled respiration was then maximized with convergent electron input through complex I and complex II by adding succinate (10 mmol l^{-1}). Finally, the chemical uncoupler carbonylcyanide-4-(trifluoromethoxy)-phenylhydrazone was titrated to assess the maximal capacity of the electron transport chain (state 3u respiration). The integrity of the outer mitochondrial membrane was assessed by the addition of cytochrome *c* (10 µmol l^{-1}) upon maximal coupled respiration. If cytochrome *c* increased oxygen consumption >15%, then the measurement was excluded to assure the viability and quality of the respiration measurement. All measurements were performed in quadruplicate.

Mitochondrial content. Mitochondrial content was assessed by mitochondrial OXPHOS protein expression using western blot analyses in BioPlex lysates of human muscle tissue as previously described[69]. Equal amounts of protein were loaded onto 4–12% Bolt gradient gels (Novex, Thermo Fisher Scientific). Proteins were transferred to a nitrocellulose membrane using the Trans-Blot Turbo transfer system (Bio-Rad Laboratories). Primary antibodies contained a cocktail of mouse monoclonal antibodies directed against structural subunits of human OXPHOS (dilution 1:10,000; ab110411, Abcam). Human OXPHOS proteins were detected using secondary antibodies conjugated with IRDye680 or IRDye800 and quantified with a CLx Odyssey near-infrared imager (LI-COR).

Magnetic resonance imaging and spectroscopy (PCr recovery and muscle volume). All magnetic resonance experiments were performed on a 3T whole-body magnetic resonance imaging scanner (Achieva 3T-X, Philips Healthcare). Participants were positioned supine in the magnetic resonance scanner to determine muscle volume with a series of T1-weighted images of the upper leg (slice thickness = 10.0 mm, no gap between slices, in-plane resolution = 0.78 × 0.78 mm). A custom-written MATLAB 2016a script (MathWorks) was used to segment adipose tissue and muscle and quantify muscle volume semiautomatically. The muscle segmentation was performed in consecutive slices between the lower end of the m. rectus femoris and the lower end of the *m*. gluteus maximus. Phosphorus magnetic resonance spectroscopy (^{31}P-MRS) was performed to measure in vivo mitochondrial function in m. vastus lateralis, as previously described[70], using a 6-cm surface coil. A series of 150 unlocalized ^{31}P spectra were acquired using the following parameters: single acquisitions (no averaging of spectra), repetition time = 4,000 ms, spectral bandwidth = 3,000 Hz, number of points = 1,024. The 150 spectra were divided into 10 spectra at rest, 70 spectra during knee-extension exercise and 70 spectra during recovery. Exercise within the scanner was performed to an auditory cue (0.5 Hz) in a custom-built knee-extension device with adjustable weight. The intensity was chosen to correspond to 50–60% of the predetermined maximum weight. Spectra were analyzed with a custom-made MATLAB 2016a script. PCr, ATP and inorganic phosphate peaks were fitted, and pH was determined. The PCr recovery was fitted with a monoexponential function, and the rate constant (k in s^{-1}) was determined as previously described[70]. The rate constant k of PCr resynthesis is almost entirely dependent on ATP produced by OXPHOS and can be used as a parameter of in vivo oxidative capacity[71].

Muscle function (exercise efficiency). Exercise efficiency was measured during a 1-h submaximal exercise bout in the fasted state on an electronically braked cycle ergometer. The submaximal cycle test was performed at 50% of maximal power output (W_{max}), as determined during a maximal aerobic cycling test. To calculate exercise energy expenditure (EEE), O_2 consumption and CO_2 production were recorded using indirect calorimetry for 15 min at two time points, $t = 15$ and $t = 45$ (Omnical, IDEE). EEE was calculated as the average of $t = 15$ and $t = 45$. Before the submaximal exercise test, resting energy expenditure (REE) was measured using indirect calorimetry. The Weir equation[72] was used to calculate whole-body energy expenditure (EE). Net energy efficiency was computed as power output (watts converted to kJ min^{-1}) over EE during exercise (EEE) minus resting EE (REE) (equation (1)) as described by Matomäkiet al.[73]:

$$NEE\,(\%) = (\text{work (kJ/min)}) \,/\, (EEE\,(\text{kJ/min}) - REE\,(\text{kJ/min})) * 100 \qquad (.1)$$

Muscle strength. Muscle contractile performance was measured using the Biodex System 3 Pro dynamometer (Biodex Medical Systems). The participants were stabilized in the device with shoulder, leg and abdominal straps to prevent compensatory movement for the measurements. The test was performed with the left leg in all participants. To measure maximal muscle strength, each participant performed 30 consecutive knee-extension and flexion movements (range of motion 120 degrees per second). The peak torque of each extension and flexion was recorded. The maximal isokinetic knee-extensor and knee-flexor torque was defined as the highest peak torque and corrected for body weight (Nm kg^{-1}) and muscle volume (Nm m^{-3}).

Habitual physical activity. Habitual physical activity was determined in all participants using an ActivPAL monitor (PAL Technologies) for a consecutive period of 5 days, including two weekend days. Besides the total amount of steps per day, the total stepping time was calculated in proportion to waking time, determined according to van der Berg et al.[74]. Stepping time (i. e., physical activity) was then further classified into high-intensity physical activity (minutes with a

step frequency >110 steps per minute in proportion to waking time) and lower-intensity physical activity (LPA; minutes with a step frequency ≤110 steps per minute in proportion to waking time)[38].

Metabolomics. Metabolomics was performed as previously described, with minor adjustments[75]. In a 2-ml tube, the following amounts of internal standard dissolved in water were added to each sample of approximately 5 mg freeze-dried muscle tissue: adenosine-$^{15}N_5$-monophosphate (5 nmol), adenosine-$^{15}N_5$-triphosphate (5 nmol), D_4-alanine (0.5 nmol), D_7-arginine (0.5 nmol), D_3-aspartic acid (0.5 nmol), D_3-carnitine (0.5 nmol), D_4-citric acid (0.5 nmol), $^{13}C_1$-citrulline (0.5 nmol), $^{13}C_6$-fructose-1,6-diphosphate (1 nmol), guanosine-$^{15}N_5$-monophosphate (5 nmol), guanosine-$^{15}N_5$-triphosphate (5 nmol), $^{13}C_6$-glucose (10 nmol), $^{13}C_6$-glucose-6-phosphate (1 nmol), D_3-glutamic acid (0.5 nmol), D_5-glutamine (0.5 nmol), D_5-glutathione (1 nmol), $^{13}C_6$-isoleucine (0.5 nmol), D_3-lactic acid (1 nmol), D_3-leucine (0.5 nmol), D_4-lysine (0.5 nmol), D_3-methionine (0.5 nmol), D_6-ornithine (0.5 nmol), D_5-phenylalanine (0.5 nmol), D_7-proline (0.5 nmol), $^{13}C_3$-pyruvate (0.5 nmol), D_3-serine (0.5 nmol), D_6-succinic acid (0.5 nmol), D5-tryptophan (0.5 nmol), D_4-tyrosine (0.5 nmol) and D_8-valine (0.5 nmol). After adding the internal standard mix, a 5-mm stainless-steel bead and polar phase solvents (for a total of 500 µl water and 500 µl MeOH) were added and samples were homogenized using TissueLyser II (Qiagen) for 5 min at a frequency of 30 times per second. Chloroform was added for a total of 1 ml to each sample before thorough mixing. Samples were then centrifuged for 10 min at 18.000 *g*. The top layer, containing the polar phase, was transferred to a new 1.5-ml tube and dried using a vacuum concentrator at 60 °C. Dried samples were reconstituted in 100 µl 3:2 (v/v) methanol/water. Metabolites were analyzed using a Waters Acquity ultrahigh-performance liquid chromatography system coupled to a Bruker Impact II ultrahigh-resolution Qq time-of-flight mass spectrometer. Samples were kept at 12 °C during analysis, and 5 µl of each sample was injected. Chromatographic separation was achieved using a Merck Millipore SeQuant ZIC-cHILIC column (Polyetheretherketone (PEEK) 100 × 2.1 mm, 3 µm particle size). Column temperature was held at 30 °C. Mobile phase consisted of (A) 1:9 (v/v) acetonitrile/water and (B) 9:1 (v/v) acetonitrile/water, both containing 5 mmol l^{-1} ammonium acetate. Using a flow rate of 0.25 ml min^{-1}, the liquid chromatography gradient consisted of 100% B for 0–2 min, reach 0% B at 28 min, 0% B for 28–30 min, reach 100% B at 31 min and 100% B for 31–32 min. Column re-equilibration was achieved at a flow rate of 0.4 ml min^{-1} at 100% B for 32–35 min. Mass spectrometry data were acquired using negative and positive ionization in full scan mode over the range of m/z 50–1,200. Data were analyzed using Bruker TASQ software version 2.1.22.3. All reported metabolite intensities were normalized to dry tissue weight, as well as to internal standards with comparable retention times and response in the mass spectrometry. Metabolite identification has been based on a combination of accurate mass, (relative) retention times and fragmentation spectra compared to the analysis of a library of standards (MSMLS, Sigma-Aldrich). General repeatability of metabolite analysis was assessed for each metabolite using repeated measurements of a pooled sample. Additionally, all peak integrations were manually checked for quality in each sample, as large natural variance may skew pooled sample results. For the detection of NAD^+ specifically, our mass spectrometry semiquantification is based on correction for a nitrogen ($^{15}N_5$)-labeled ATP internal standard. Both NAD^+ and ATP contain several phosphate groups and the adenosine scaffold and thus behave in a very similar way throughout sample preparation; furthermore, their retention times in the mass spectrometer are generally within 1 min of one another, making it more likely that they encounter similar matrix effects in mass spectrometry. We have previously demonstrated that this approach gives results equivalent to those obtained using a dedicated enzymatic method for absolute NAD^+ quantification[27,76].

Statistical analyses and data visualization. Data were processed and analyses were performed with R version 3.5.1 (ref. [77]) and Bioconductor version 3.7[78]. Data were processed in part with the R package dplyr version 1.0.2 (ref. [79]). Principal-component analysis was performed using the R package MixOmics version 6.6.2 (ref. [80]). Significance was assessed using an empirical Bayes moderated *t* test on log_2-transformed data within limma's linear model framework, taking participant groups into account[81,82]. Networks were constructed and visualized using igraph version 1.2.4.2 (ref. [83]). Unless implemented through an aforementioned R package or base R graphics, visualization of data was performed using ggplot2 version 3.2.1 (ref. [84]), ggpubr v 0.2.5 (ref. [85]) and ggrepel version 0.8.1 (ref. [86]), with colors from RColorBrewer version 1.1-2 (ref. [87]).

Reporting Summary. Further information on research design is available in the Nature Research Reporting Summary linked to this article.

Data availability

Metabolomics data are available as supplementary materials accompanying this article as both summary statistics and processed abundance values per individual (statistical Source Data). Physiological data from this cohort have been reported in our previous study as part of a different analysis[25]. All other data supporting the findings of this study are available from the corresponding author upon reasonable request.

Code availability

Code supporting the findings of this study are available from the corresponding author upon reasonable request

Received: 26 May 2021; Accepted: 12 January 2022;
Published online: 17 February 2022

References

1. Salomon, J. A. et al. Healthy life expectancy for 187 countries, 1990–2010: a systematic analysis for the Global Burden Disease Study 2010. *Lancet* **380**, 2144–2162 (2012).
2. Ferrucci, L. et al. Epidemiology of aging. *Radiol. Clin. North Am.* **46**, 643–652 (2008).
3. Butler, R. N. et al. New model of health promotion and disease prevention for the 21st century. *BMJ.* **337**, a399 (2008).
4. Niccoli, T. & Partridge, L. Ageing as a risk factor for disease. *Curr. Biol.* **22**, R741–R752 (2012).
5. López-Otín, C., Blasco, M. A., Partridge, L., Serrano, M. & Kroemer, G. The hallmarks of aging. *Cell* **153**, 1194–1217 (2013).
6. Houtkooper, R. H. et al. The metabolic footprint of aging in mice. *Sci. Rep.* **1**, 134 (2011).
7. Uchitomi, R. et al. Metabolomic analysis of skeletal muscle in aged mice. *Sci. Rep.* **9**, 10425 (2019).
8. Gao, A. W. et al. A sensitive mass spectrometry platform identifies metabolic changes of life history traits in *C. elegans*. *Sci. Rep.* **7**, 2408 (2017).
9. Roubenoff, R. Sarcopenia and its implications for the elderly. *Eur. J. Clin. Nutr.* **54**, S40–S47 (2000).
10. Janssen, I. et al. Low relative skeletal muscle mass (sarcopenia) in older persons is associated with functional impairment and physical disability. *J. Am. Geriatr. Soc.* **50**, 889–896 (2002).
11. Distefano, G. et al. Physical activity unveils the relationship between mitochondrial energetics, muscle quality, and physical function in older adults. *J. Cachexia. Sarcopenia Muscle* **9**, 279–294 (2018).
12. Talbot, L. A. et al. Falls in young, middle-aged and older community dwelling adults: perceived cause, environmental factors and injury. *BMC Public Health* **5**, 86 (2005).
13. Gadelha, A. B. et al. The relationship between muscle quality and incidence of falls in older community-dwelling women: an 18-month follow-up study. *Exp. Gerontol.* **110**, 241–246 (2018).
14. Fried, L. P. et al. Frailty in older adults: evidence for a phenotype. *J. Gerontol. A Biol. Sci. Med. Sci.* **56**, M146–M156 (2001).
15. Amati, F. et al. Physical inactivity and obesity underlie the insulin resistance of aging. *Diabetes Care* **32**, 1547–1549 (2009).
16. Riera, C. E. & Dillin, A. Tipping the metabolic scales towards increased longevity in mammals. *Nat. Cell Biol.* **17**, 196–203 (2015).
17. Romani, M. et al. NAD^+ boosting reduces age-associated amyloidosis and restores mitochondrial homeostasis in muscle. *Cell Rep.* **34**, 108660 (2021).
18. Cartee, G. D., Hepple, R. T., Bamman, M. M. & Zierath, J. R. Exercise promotes healthy aging of skeletal muscle. *Cell Metab.* **23**, 1034–1047 (2016).
19. Greggio, C. et al. Enhanced respiratory chain supercomplex formation in response to exercise in human skeletal muscle. *Cell Metab.* **25**, 301–311 (2017).
20. Soga, T. et al. Differential metabolomics reveals ophthalmic acid as an oxidative stress biomarker indicating hepatic glutathione consumption. *J. Biol. Chem.* **281**, 16768–16776 (2006).
21. Dello, S. A. W. D. et al. Systematic review of ophthalmate as a novel biomarker of hepatic glutathione depletion. *Clin. Nutr.* **32**, 325–330 (2013).
22. Smith, K. R. et al. Dihydroxyacetone exposure alters NAD(P)H and induces mitochondrial stress and autophagy in HEK293T cells. *Chem. Res. Toxicol.* **32**, 1722–1731 (2019).
23. Gluck, M. R. & Zeevalk, G. D. Inhibition of brain mitochondrial respiration by dopamine and its metabolites: implications for Parkinson's disease and catecholamine-associated diseases. *J. Neurochem.* **91**, 788–795 (2004).
24. Wirthgen, E. et al. The Janus-faced role of an immunomodulatory tryptophan metabolite and its link to pathological conditions. *Front. Immunol.* **8**, 1957 (2018).
25. Grevendonk, L. et al. Impact of aging and exercise on skeletal muscle mitochondrial capacity, energy metabolism, and physical function. *Nat. Commun.* **12**, 1–17 (2021).
26. Rajman, L. et al. Therapeutic potential of NAD-boosting molecules: the in vivo evidence. *Cell Metab.* **27**, 529–547 (2018).
27. Remie, C. M. E. et al. Nicotinamide riboside supplementation alters body composition and skeletal muscle acetylcarnitine concentrations in healthy obese humans. *Am. J. Clin. Nutr.* **112**, 413–426 (2020).
28. Pirinen, E. et al. Niacin cures systemic NAD^+ deficiency and improves muscle performance in adult-onset mitochondrial myopathy. *Cell Metab.* **31**, 1078–1090 (2020).

29. Elhassan, Y. S. et al. Nicotinamide riboside augments the aged human skeletal muscle NAD^+ metabolome and induces transcriptomic and anti-inflammatory signatures. *Cell Rep.* **28**, 1717–1728 (2019).
30. Cantó, C. et al. The NAD^+ precursor nicotinamide riboside enhances oxidative metabolism and protects against high-fat diet-induced obesity. *Cell Metab.* **15**, 838–847 (2012).
31. Sorrentino, V. et al. Enhancing mitochondrial proteostasis reduces amyloid-β proteotoxicity. *Nature* **552**, 187–193 (2017).
32. Zhang, H. et al. NAD^+ repletion improves mitochondrial and stem cell function and enhances life span in mice. *Science* **352**, 1436–1443 (2016).
33. Gomes, A. P. et al. Declining NAD^+ induces a pseudohypoxic state disrupting nuclear-mitochondrial communication during aging. *Cell* **155**, 1624–1638 (2013).
34. Mills, K. F. Long-term administration of nicotinamide mononucleotide mitigates age-associated physiological decline in mice. *Cell Metab.* **24**, 795–806 (2016).
35. Yoshino, J. et al. Nicotinamide mononucleotide, a key NAD^+ intermediate, treats the pathophysiology of diet- and age-induced diabetes in mice. *Cell Metab.* **14**, 528–536 (2011).
36. Mouchiroud, L. et al. The NAD^+/sirtuin pathway modulates longevity through activation of mitochondrial UPR and FOXO signaling. *Cell* **154**, 431–441 (2013).
37. Connell, N. J. et al. NAD^+ metabolism as a target for metabolic health: have we found the silver bullet? *Diabetologia* **62**, 888–899 (2019).
38. Tudor-Locke, C. et al. How many steps/day are enough? For adults. *Int. J. Behav. Nutr. Phys. Act.* **8**, 79 (2011).
39. Tudor-Locke, C. et al. Revisiting 'how many steps are enough?' *Med. Sci. Sports Exerc.* **40**, S537–S543 (2008).
40. Zhu, X. H. et al. In vivo NAD assay reveals the intracellular NAD contents and redox state in healthy human brain and their age dependences.*Proc. Natl. Acad. Sci. USA* **112**, 2876–2881 (2015).
41. Cuenoud, B. et al. Brain NAD is associated with ATP energy production and membrane phospholipid turnover in humans.*Front. Aging Neurosci.* **12**, 609517 (2020).
42. Massudi, H. et al. Age-associated changes in oxidative stress and NAD^+ metabolism in human tissue. *PLoS One* **7**, e42357.
43. de Guia, R. M. et al. Aerobic and resistance exercise training reverses age-dependent decline in NAD^+ salvage capacity in human skeletal muscle.*Physiol. Rep.* **7**, e14139 (2019).
44. Drummond, M. J. et al. Aging and microRNA expression in human skeletal muscle: a microarray and bioinformatics analysis.*Physiol. Genomics* **43**, 595–603 (2011).
45. Fazelzadeh, P. et al. The muscle metabolome differs between healthy and frail older adults.*J. Proteome Res.* **15**, 499–509 (2016).
46. Rivas, D. A. et al. Diminished skeletal muscle microRNA expression with aging is associated with attenuated muscle plasticity and inhibition of IGF-1 signaling. *FASEB J.* **28**, 4133–4147 (2014).
47. Migliavacca, E. et al. Mitochondrial oxidative capacity and NAD^+ biosynthesis are reduced in human sarcopenia across ethnicities.*Nat. Commun.* **10**, 5808 (2019).
48. Costford, S. R. et al. Skeletal muscle NAMPT is induced by exercise in humans.*Am. J. Physiol. Endocrinol. Metab.* **298**, E117–E126 (2010).
49. Zha, M. et al. Molecular mechanism of ADP-ribose hydrolysis by human NUDT5 from structural and kinetic studies.*J. Mol. Biol.* **379**, 568–578 (2008).
50. Perraud, A. L. et al. NUDT9, a member of the Nudix hydrolase family, is an evolutionarily conserved mitochondrial ADP-ribose pyrophosphatase.*J. Biol. Chem.* **278**, 1794–1801 (2003).
51. Hove-Jensen, B. et al. Phosphoribosyl diphosphate (PRPP): biosynthesis, enzymology, utilization, and metabolic significance.*Microbiol. Mol. Biol. Rev.* **81**, e00040-16 (2017).
52. Kepplinger, B. et al. Age-related increase of kynurenic acid in human cerebrospinal fluid: IgG and β2-microglobulin changes.*Neurosignals* **14**, 126–135 (2005).
53. Vohra, M. et al. Kynurenic acid accumulation underlies learning and memory impairment associated with aging.*Genes Dev.* **32**, 14–19 (2018).
54. Calder, P. et al. Health relevance of the modification of low-grade inflammation in ageing (inflammageing) and the role of nutrition. *Ageing Res. Rev.* **40**, 95–119 (2017).
55. Lim, A. et al. Does exercise influence kynurenine/tryptophan metabolism and psychological outcomes in persons with age-related diseases? A systematic review. *Int. J. Tryptophan Res.* **14**, 1178646921991119 (2021).
56. Sorgdrager, F. J. H. et al. Tryptophan metabolism in inflammaging: from biomarker to therapeutic target. *Front. Immunol.* **10**, 2565 (2019).
57. Agudelo, L. Z. et al. Skeletal muscle PGC-1α1 reroutes kynurenine metabolism to increase energy efficiency and fatigue-resistance.*Nat. Commun.* **10**, 2767 (2019).
58. Yoshino, M. et al. Nicotinamide mononucleotide increases muscle insulin sensitivity in prediabetic women.*Science* **372**, 1224–1229 (2021).
59. Moore, P. & Mucinski, J. M. Impact of nicotinamide riboside supplementation on skeletal muscle mitochondria and whole-body glucose homeostasis: challenging the current hypothesis.*J. Physiol.* **598**, 3327–3328 (2020).
60. Aagaard, P. et al. Mechanical muscle function, morphology, and fiber type in lifelong trained elderly.*Med. Sci. Sports Exerc.* **39**, 1989–1996 (2007).
61. Mackey, A. L. et al. Differential satellite cell density of type I and II fibres with lifelong endurance running in old men.*Acta Physiol.* **210**, 612–627 (2014).
62. Mosole, S. et al. Long-term high-level exercise promotes muscle reinnervation with age.*J. Neuropathol. Exp. Neurol.* **73**, 284–294 (2014).
63. Di Lisa, F. & Ziegler, M. Pathophysiological relevance of mitochondria in NAD^+ metabolism. *FEBS Lett.* **492**, 4–8 (2001).
64. Guralnik, J. M. et al. A short physical performance battery assessing lower extremity function: association with self-reported disability and prediction of mortality and nursing home admission.*J. Gerontol.* **49**, M85–M94 (1994).
65. Bergström, J. et al. Diet, muscle glycogen and physical performance.*Acta Physiol. Scand.* **71**, 140–150 (1967).
66. Phielix, E. et al. Lower intrinsic ADP-stimulated mitochondrial respiration underlies in vivo mitochondrial dysfunction in muscle of male type 2 diabetic patients. *Diabetes* **57**, 2943–2949 (2008).
67. Boushel, R. et al. Patients with type 2 diabetes have normal mitochondrial function in skeletal muscle.*Diabetologia* **50**, 790–796 (2007).
68. Hoeks, J. et al. Prolonged fasting identifies skeletal muscle mitochondrial dysfunction as consequence rather than cause of human insulin resistance.*Diabetes* **59**, 117–125 (2010).
69. van Moorsel, D. et al. Demonstration of a day-night rhythm in human skeletal muscle oxidative capacity.*Mol. Metab.* **5**, 635–645 (2016).
70. Schrauwen-Hinderling, V. B. et al. Impaired in vivo mitochondrial function but similar intramyocellular lipid content in patients with type 2 diabetes mellitus and BMI-matched control subjects. *Diabetologia* **50**, 113–120 (2007).
71. Kemp, G. J. & Radda, G. K. Quantitative interpretation of bioenergetic data from 31P and 1H magnetic resonance spectroscopic studies of skeletal muscle: an analytical review.*Magn. Reson. W.* **10**, 43–63 (1994).
72. Weir, J. B. d. V. et al. New methods for calculating metabolic rate with special reference to protein metabolism.*J. Physiol.* **109**, 1–9 (1949).
73. Matomäki, P. A comparison of methodological approaches to measuring cycling mechanical efficiency.*Sports Med. Open* **5**, 23 (2019).
74. van der Berg, J. D. et al. Identifying waking time in 24-h accelerometry data in adults using an automated algorithm.*J. Sports Sci.* **34**, 1867–1873 (2016).
75. Molenaars, M. et al. A conserved mito-cytosolic translational balance links two longevity pathways.*Cell Metab.* **31**, 549–563 (2020).
76. Zapata-Pérez, R. et al. Reduced nicotinamide mononucleotide is a new and potent NAD+ precursor in mammalian cells and mice.*FASEB J.* **35**, e21456 (2021).
77. The R Development Core Team. R: a language and environment for statistical computing (R Foundation for Statistical Computing, 2010).
78. Gentleman, R. C. et al. Bioconductor: open software development for computational biology and bioinformatics.*Genome Biol.* **5**, R80 (2004).
79. Wickham, H., François, R., Henry, L. & Müller, K. dplyr: a grammar of data manipulation. R package version (Media, 2019).
80. Rohart, F., Gautier, B., Singh, A. & Lê Cao, K. A. mixOmics: an R package for 'omics feature selection and multiple data integration. *PLoS Comput. Biol.* **13**, e1005752 (2017).
81. Ritchie, M. E. et al. limma powers differential expression analyses for RNA-sequencing and microarray studies. *Nucleic Acids Res.* **43**, e47 (2015).
82. Law, C. W., Chen, Y., Shi, W. & Smyth, G. K. voom: precision weights unlock linear model analysis tools for RNA-seq read counts. *Genome Biol.* **15**, R29 (2014).
83. Csardi, G. & Nepusz, T. The igraph software package for complex network research. *Int. J. Complex Syst.* **1695**, 1–9 (2006).
84. Wickham, H. Ggplot2. *Wiley Interdiscip. Rev. Comput. Stat.* **3**, 180–185 (2011).
85. Kassambara, A. Package 'ggpubr': 'ggplot2' based publication ready plots. R package v.0.4.0 (2020).
86. Slowikowski, K. ggrepel: automatically position non-overlapping text labels with 'ggplot2'. R package v.0.8.2 (2020).
87. Neuwirth, E. RColorBrewer: ColorBrewer palettes. R package v.1.1-2 (2014).

Acknowledgements

L.G., J.H. and P.S. are financially supported by the TI Food and Nutrition (TIFN) research program Mitochondrial Health (ALWTF.2015.5) and the Netherlands Organization for Scientific Research. Work in the Houtkooper group is financially supported by the European Research Council (starting grant 638290), ZonMw (Vidi grant 91715305) and Velux Stiftung (grant 1063). G.E.J. is supported by a Veni grant from ZonMw and an Amsterdam Gastroenterology Endocrinology Metabolism (AGEM) Talent grant. R.Z.P. is supported by a postdoctoral grant from the European Union's Horizon 2020 research and innovation program under Marie Skłodowska-Curie grant agreement 840110. The funders had no role in data collection and analysis or decision to publish.

Author contributions

G.E.J., L.G., P.S., J.H. and R.H.H. conceived the study. L.G. designed and performed the human cohort characterization and experiments. G.E.J. designed and performed the bioinformatics analyses. R.Z.P., B.V.S., and M.v.W. performed the metabolomics analyses. J.M.W.G. and J.d.V.-v.d.B. reviewed the manuscript. G.E.J., L.G., R.Z.P., B.V.S., P.S., R.H.H. and J.H. interpreted the results and wrote the manuscript with contributions from all other authors.

Competing interests

J.M.W.G. and J.d.V.-v.d.B. are affiliated with FrieslandCampina and Danone Nutricia Research, respectively, which sponsored the TI Food and Nutrition (TIFN) program and partly financed the project that led to human sample collection. They had no role in data collection, analysis, or decision to publish. The remaining authors declare no competing interests.

Additional information

Extended data is available for this paper at https://doi.org/10.1038/s43587-022-00174-3.

Supplementary information The online version contains supplementary material available at https://doi.org/10.1038/s43587-022-00174-3.

Correspondence and requests for materials should be addressed to Riekelt H. Houtkooper or Joris Hoeks.

Peer review information *Nature Aging* thanks Nicholas Rattray, Paul Coen, and the other, anonymous, reviewer(s) for their contribution to the peer review of this work.

Reprints and permissions information is available at www.nature.com/reprints.

Publisher's note Springer Nature remains neutral with regard to jurisdictional claims in published maps and institutional affiliations.

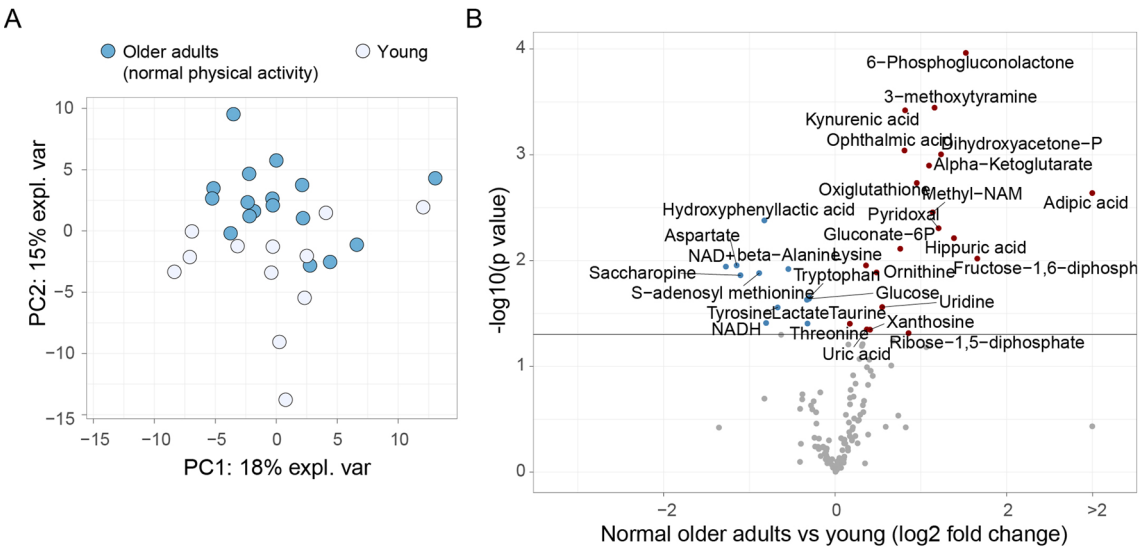

Extended Data Fig. 1 | Global metabolomics changes of human muscle aging. (**a**) Principal Component Analysis (PCA) of metabolomes of young and older individuals possessing equal physical activity levels ('young' vs 'normal older adults'). (**b**) Volcano plot of fold change (x axis, log2 scale) versus p value (y axis, -log10 scale) for older adults (n = 17) compared to young individuals (n = 12) with equal physical activity levels, illustrating significantly lower (blue) or higher (red) metabolites with age. The horizontal line indicates significance ($p < 0.05$). Significance was determined using an empirical Bayes moderated t test (two-sided, p values adjusted for multiple comparisons between groups). Source data: Statistical_Source_Data.csv, all exact p values for comparison between groups are listed therein.

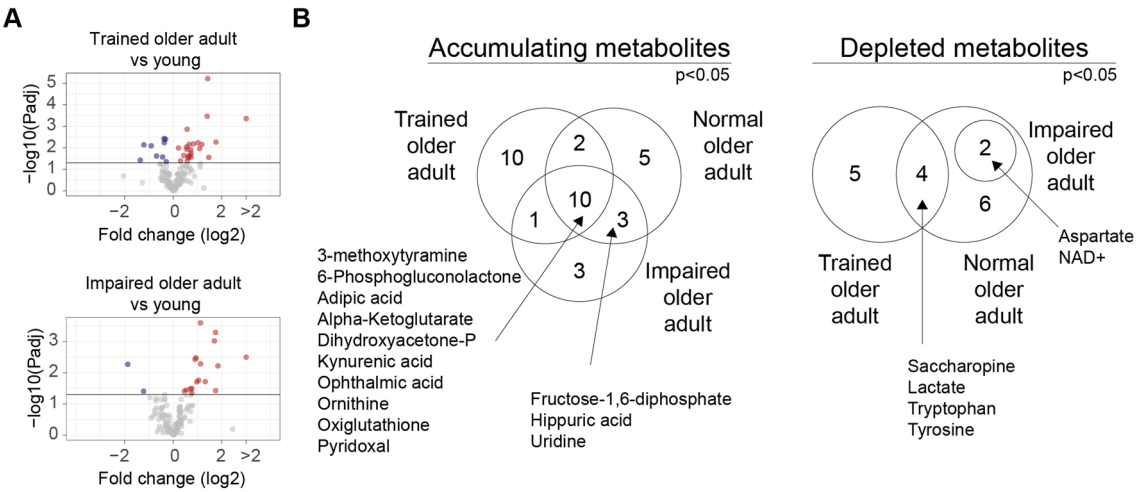

Extended Data Fig. 2 | Comparison of age-related changes in each age group. (**a**) Volcano plots of fold change (x axis, log2 scale) versus p value (y axis, -log10 scale) for trained older adults (top; n = 17), and physically impaired older adults (bottom; n = 6) compared to young individuals (n = 12), illustrating significantly depleted (blue) or accumulated (red) metabolites with age. Line indicates significance ($p < 0.05$). Significance was determined using an empirical Bayes moderated t test (two-sided, p values adjusted for multiple comparisons between groups). (**b**) Venn diagram of the overlap of significantly higher or lower abundances of metabolites in each aged group (trained older adults, older adults with normal physical activity levels, physically impaired older adults) compared to young individuals ($p < 0.05$). Source data: Statistical_Source_Data.csv, all exact p values for comparison between groups are listed therein.

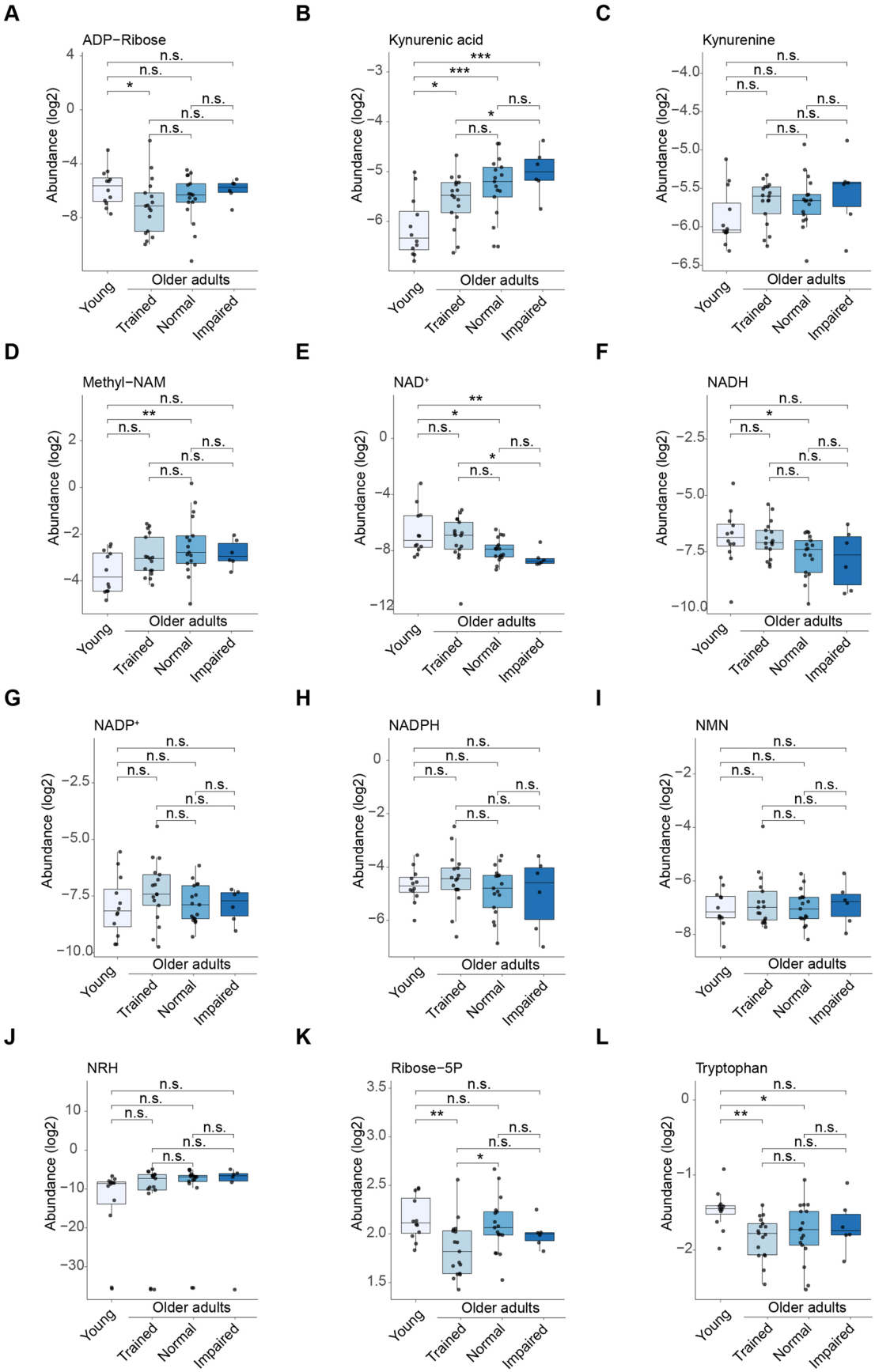

Extended Data Fig. 3 | See next page for caption.

Extended Data Fig. 3 | NAD$^+$-related metabolites of healthy aging groups. (**a**-**l**) Abundance levels of NAD + -related metabolites in the four muscle health groups, for (A) ADP-ribose, (B) Kynurenic acid, (C) Kynurenine, (D) Methyl-NAM, (E) NAD +, (F) NADH, (G) NADP +, (H) NADPH, (I) Nicotinamide mononucleotide (NMN), (J) Dihydronicotinamide riboside (NRH), (K) Ribose-5P, and (L) Tryptophan. Sample sizes are: young n = 12, older adults; trained n = 17, Normal=17, impaired=6. Significance was determined using an empirical Bayes moderated t test (two-sided, p values adjusted for multiple comparisons between groups, * $p < 0.05$, ** $p < 0.01$, *** $p < 0.001$, n.s. = not significant). Boxplots: Inner line within the box is the median of the data, the box extends to the upper and lower quartile of the dataset (25% of the data above and below the median), whiskers (dashed lines) represent up to 1.5 times the upper or lower quartiles, circles beyond the whisker represent individual data points outside this range. Source data: Statistical_Source_Data.csv, all exact p values for comparison between groups are listed therein.

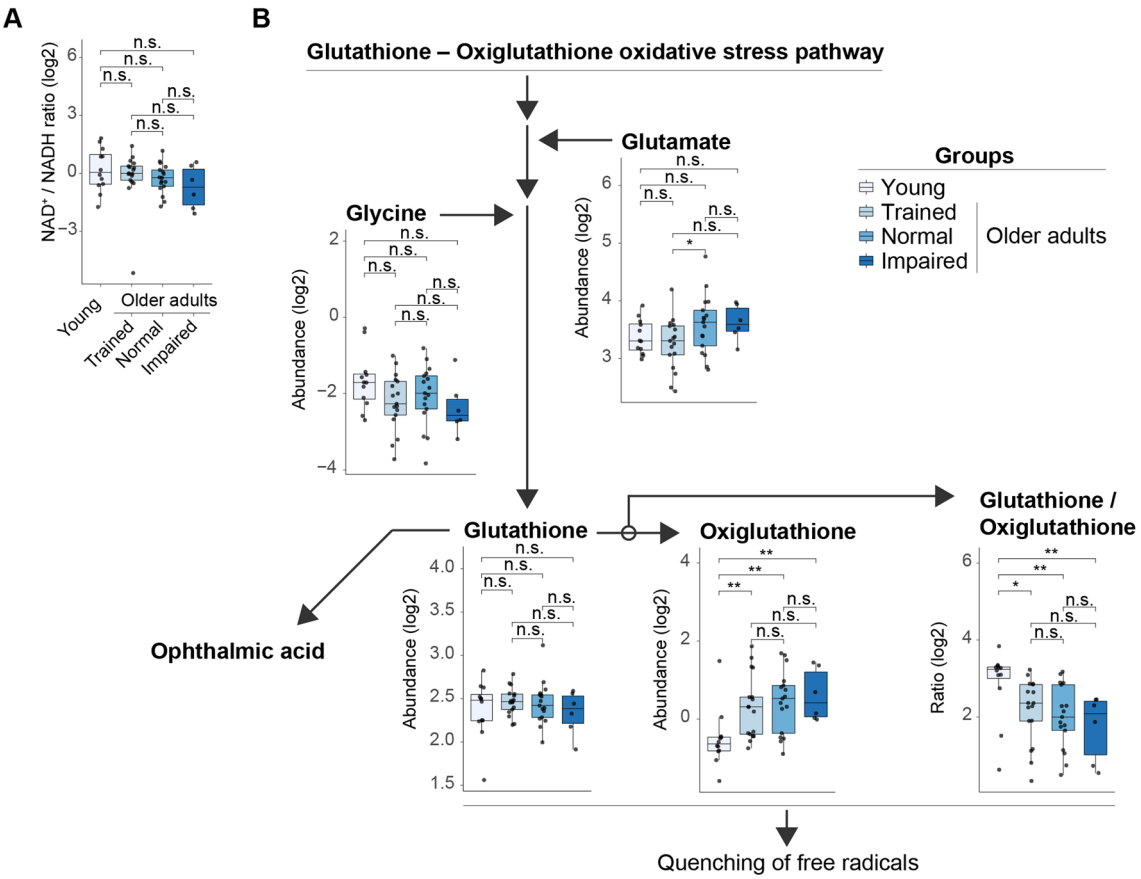

Extended Data Fig. 4 | NAD$^{+/}$ NADH ratio, and the glutathione/oxiglutathion oxidative stress pathway. (**a**) NAD + to NADH ratio (log2 scale) in young and older adults belonging to trained, normal, and impaired aging groups. (**b**) The glutathione – oxliglutathione oxidative stress pathway for metabolites measured in this study. Glutamate and glycine feed into glutathione production. Conversion of glutathione to oxiglutathione results in quenching of free radicals, whereby the ratio of glutathione to oxiglutathione is indicative of this process. A byproduct of this pathway is ophthalmic acid (data presented in Fig. 2c). Data suggests an increase of the oxidative milieu in the aged groups relative to young. Sample sizes are: young n = 12, older adults; trained n = 17, Normal=17, impaired=6. Significance was determined using an empirical Bayes moderated t test (two-sided, p values adjusted for multiple comparisons between groups, * $p < 0.05$, ** $p < 0.01$, n.s. = not significant). Boxplots: Inner line within the box is the median of the data, the box extends to the upper and lower quartile of the dataset (25% of the data above and below the median), whiskers (dashed lines) represent up to 1.5 times the upper or lower quartiles, circles beyond the whisker represent individual data points outside this range. Source data: Statistical_Source_Data.csv, all exact p values for comparison between groups are listed therein.

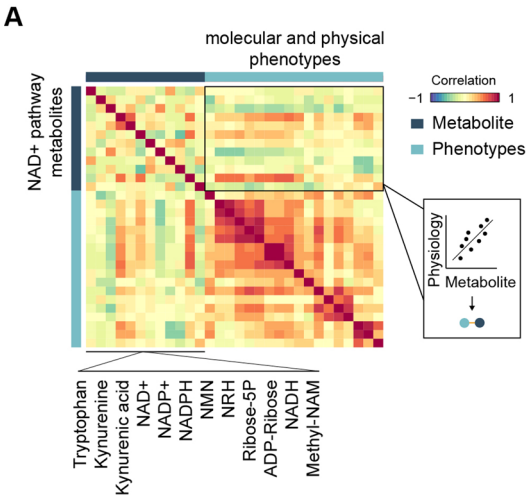

B

Node	Measurement
Mu.Function	Muscle function - Net exercise efficiency (%)
Mito.1	Mitochondria - OXPHOS compl V blot (A.U.)
Mito.2	Mitochondria - OXPHOS compl III blot (A.U.)
Mito.3	Mitochondria - OXPHOS compl II blot (A.U.)
Mito.4	Mitochondria - OXPHOS compl IV blot (A.U.)
Mito.5	Mitochondria - OXPHOS compl I blot (A.U.)
Resp.1	Respiration - Coupled MOGS3 (pmol/(s*mg))
Resp.2	Respiration - Uncoupled MOGS (pmol/(s*mg))
Resp.3	Respiration - Coupled MGS3 (pmol/(s*mg))
Mito.Function	Mitochondrial function - MRS PCr recovery rate
Mu.Mass	Muscle mass - MRI Muscle volume (cm3)
Mu.Strength1	Muscle isokinetic extension / body weight (Nm/kg)
Mu.Strength2	Muscle isokinetic extension / muscle volume (Nm/cm3)
Mu.Strength3	Muscle isokinetic flexion / body weight (Nm/kg)
Mu.Strength4	Muscle isokinetic flexion / muscle volume (Nm/cm3)
PA.1	Physical activity - steps per day
PA.2	Physical activity- % time high physical activity
PA.3	Physical activity- % time low physical activity

Extended Data Fig. 5 | Correlation of molecular–physiological phenotypes with metabolites involved in NAD$^+$ synthesis. (**a**) Correlation matrix comparing the paired metabolome (dark blue) and muscle health parameters (light blue) in the older adults (Pearson's product-moment correlation coefficient, sample size is all older adults, n = 40). The scale ranges from blue (negative correlation), to yellow (no correlation), to red (positive correlation). Inset and cartoon: correlation between metabolites and muscle health parameters are used to reconstruct the network. (**b**) Abbreviations and measurements of the molecular-physiological phenotypes assessed in this analysis. Note: MOGS3, state 3 respiration upon malate + octanoyl-carnitine + glutamate + succinate, MGS3, state 3 respiration upon malate + glutamate + succinate. Source data: Statistical_Source_Data.csv and physiological data is available in our previous study[25].

nature portfolio

Corresponding author(s): Riekelt H. Houtkooper, Joris Hoeks

Last updated by author(s): Dec 10, 2021

Reporting Summary

Nature Portfolio wishes to improve the reproducibility of the work that we publish. This form provides structure for consistency and transparency in reporting. For further information on Nature Portfolio policies, see our Editorial Policies and the Editorial Policy Checklist.

Statistics

For all statistical analyses, confirm that the following items are present in the figure legend, table legend, main text, or Methods section.

n/a	Confirmed
☐	☒ The exact sample size (*n*) for each experimental group/condition, given as a discrete number and unit of measurement
☐	☒ A statement on whether measurements were taken from distinct samples or whether the same sample was measured repeatedly
☐	☒ The statistical test(s) used AND whether they are one- or two-sided *Only common tests should be described solely by name; describe more complex techniques in the Methods section.*
☐	☒ A description of all covariates tested
☐	☒ A description of any assumptions or corrections, such as tests of normality and adjustment for multiple comparisons
☐	☒ A full description of the statistical parameters including central tendency (e.g. means) or other basic estimates (e.g. regression coefficient) AND variation (e.g. standard deviation) or associated estimates of uncertainty (e.g. confidence intervals)
☐	☒ For null hypothesis testing, the test statistic (e.g. *F*, *t*, *r*) with confidence intervals, effect sizes, degrees of freedom and *P* value noted *Give P values as exact values whenever suitable.*
☒	☐ For Bayesian analysis, information on the choice of priors and Markov chain Monte Carlo settings
☒	☐ For hierarchical and complex designs, identification of the appropriate level for tests and full reporting of outcomes
☐	☒ Estimates of effect sizes (e.g. Cohen's *d*, Pearson's *r*), indicating how they were calculated

Our web collection on statistics for biologists contains articles on many of the points above.

Software and code

Policy information about availability of computer code

Data collection	Onmical Software, IDEE, Maastricht, The Netherlands
Data analysis	MATLAB 2016a for Windows Bruker TASQ software version 2.1.22.3 R version 3.5.1 Bioconductor version 3.7 R package dplyr version 1.0.2 R package MixOmics version 6.6.2 R package Limma version 3.38.3 R package igraph version 1.2.4.2 R package ggplot2 version 3.2.1 R package ggpubr v 0.2.5 R package ggrepel version 0.8.1 R package RColorBrewer version 1.1-2

For manuscripts utilizing custom algorithms or software that are central to the research but not yet described in published literature, software must be made available to editors and reviewers. We strongly encourage code deposition in a community repository (e.g. GitHub). See the Nature Portfolio guidelines for submitting code & software for further information.

Data

Policy information about availability of data

All manuscripts must include a data availability statement. This statement should provide the following information, where applicable:

- Accession codes, unique identifiers, or web links for publicly available datasets
- A description of any restrictions on data availability
- For clinical datasets or third party data, please ensure that the statement adheres to our policy

Metabolomics data are available as supplementary materials accompanying this manuscript as both summary statistics and processed abundance values per individual (Supplemental Table 2). Physiological data from this cohort has been reported in our previous study as part of a different analysis (see ref 25). All other data supporting the findings of this study are available from the corresponding author upon reasonable request.

Field-specific reporting

Please select the one below that is the best fit for your research. If you are not sure, read the appropriate sections before making your selection.

☒ Life sciences ☐ Behavioural & social sciences ☐ Ecological, evolutionary & environmental sciences

For a reference copy of the document with all sections, see nature.com/documents/nr-reporting-summary-flat.pdf

Life sciences study design

All studies must disclose on these points even when the disclosure is negative.

Sample size	For the cross-sectional study, a power calculation was performed based on the main comparison with the smallest expected difference, i.e. the difference in ex vivo mitochondrial respiration between older adults with and without a compromised physical fitness. To correct for multiple testing, the power calculation was based on a significance level (α) of 0.167 (=0.05 / 3) and a power (π) of 80%. To detect a ~15% difference in mitochondrial function; inclusion of 17 subjects per group was needed. Taking a dropout rate of 10% during the study into account, inclusion of 19 subjects per group, and a total amount of 76 subjects, was required. Due to recruitment difficulties only 6 suitable participants were included in the impaired older adults (IO) group.
Data exclusions	For a couple of parameters a number of measurements were omitted from the final data analyses due to technical issues with the measurements.
Replication	Data were not replicated due to the nature of the measurements and study design, in addition to the burden on the participants.
Randomization	As participants were allocated to the experimental groups based on age, physical activity, and physical function, randomization was not relevant in this cross-sectional study design. Participants were assigned to the following study groups: Young individuals with normal physical activity (Y, 20 – 30 years), older adults with normal physical activity (O, 65 – 80 years), trained older adults (TO, 65 – 80 years) and physically impaired older adults (IO, 65 – 80 years). Participants were considered normally physically active (O) if they completed no more than one structured exercise session per week, whereas participants were considered trained (TO) if they engaged in at least 3 structured exercise sessions of at least 1 hour each per week for an uninterrupted period of at least one year. Participants were classified as older adults with impaired physical function (IO) in case of an SPPB score of ≤ 9.
Blinding	Blinding was not possible in this study because the group allocation, the data collection and data analysis were for most of the measurements performed by the same investigator. PCr-MRS measurements, muscle volume MRI measurements, and western blots were analyzed by other investigators of the research team who were blinded for group allocations.

Reporting for specific materials, systems and methods

We require information from authors about some types of materials, experimental systems and methods used in many studies. Here, indicate whether each material, system or method listed is relevant to your study. If you are not sure if a list item applies to your research, read the appropriate section before selecting a response.

Materials & experimental systems

n/a	Involved in the study
☐	☒ Antibodies
☒	☐ Eukaryotic cell lines
☒	☐ Palaeontology and archaeology
☒	☐ Animals and other organisms
☐	☒ Human research participants
☐	☒ Clinical data
☒	☐ Dual use research of concern

Methods

n/a	Involved in the study
☒	☐ ChIP-seq
☒	☐ Flow cytometry
☒	☐ MRI-based neuroimaging

Antibodies

Antibodies used	ab110411, Abcam, Cambridge, UK; Li-COR, Westburg, Leusden, The Netherlands
Validation	Primary antibodies contained a cocktail of mouse monoclonal antibodies directed against structural subunits of human OXPHOS (dilution 1:10,000; ab110411, Abcam, Cambridge, UK). The hOxPHOS proteins were detected using secondary antibodies conjugated with IRDye680 or IRDye800 and were quantified with a CLx Odyssey Near-Infrared Imager (Li-COR, Westburg, Leusden, The Netherlands).

Human research participants

Policy information about studies involving human research participants

Population characteristics	Participants were allocated to the experimental groups based on age, physical activity, and physical function. Participants were assigned to the following study groups: Young individuals with normal physical activity (Y, 20 – 30 years), older adults with normal physical activity (O, 65 – 80 years), trained older adults (TO, 65 – 80 years) and physically impaired older adults (IO, 65 – 80 years). Participants were considered normally physically active (O) if they completed no more than one structured exercise session per week, whereas participants were considered trained (TO) if they engaged in at least 3 structured exercise sessions of at least 1 hour each per week for an uninterrupted period of at least one year. Participants were classified as older adults with impaired physical function (IO) in case of an SPPB score of ≤ 9.
Recruitment	Participants were recruited in the community of Maastricht and its surroundings through advertisements placed on the Maastricht University campus, in newspapers, supermarkets, and at sports clubs. Most of the volunteers that wanted to participate were interested in their own muscle health and as such a self-selection bias could have taken place resulting in a overall very healthy study population as reflected in the results.
Ethics oversight	The study was conducted in accordance with the principles of the declaration of Helsinki and approved by the Ethics Committee of the Maastricht University Medical Center+. All participants provided their written informed consent.

Note that full information on the approval of the study protocol must also be provided in the manuscript.

Clinical data

Policy information about clinical studies

All manuscripts should comply with the ICMJE guidelines for publication of clinical research and a completed CONSORT checklist must be included with all submissions.

Clinical trial registration	Study was registered at clinicaltrials.gov with identifier NCT03666013
Study protocol	The trial protocol can be asseced on clinicaltrails.gov and in the submitted paper
Data collection	The study was conducted at the Metabolic Research Unit within the Maastricht University Medical Centre in The Netherlands. Recruitment took place between August 2017 and January 2020. Data collection took place between September 2017 and March 2020.
Outcomes	As our primary aim was to examine to what extent physical activity contributes to the decline in mitochondrial function during aging, mitochondrial capacity was our primary outcome. Skeletal muscle mitochondrial capacity was determined both ex vivo in permeabilized muscle fibres and in vivo via non-invasive assessment of PCr recovery rates using MR spectroscopy. Furthermore we aimed to investigate to which extent this decline in mitochondrial function related to muscle health and physical function and therefore included muscle strength, muscle volume, insulin sensitivity, gait stability and adaptability, exercise capacity, and exercise efficiency as secondary outcomes. Muscle strength was measured in the upper leg using the Biodex System 3 Pro dynamometer. Muscle volume was determined in the MR scanner with a series of T1-weighted images of the upper leg. A hyperinsulinemic-euglycemic clamp was performed to assess peripheral insulin sensitivity. Walking performance and stability were assessed during a self-paced 6-minute walk test (6MWT), during multiple fixed-speed gait trials and during a repeated balance disturbance trial using a dual-belt, force plate-instrumented treadmill within a virtual environment. Maximal exercise capacity ($\dot{V}O2max$) was assessed during a graded cycling test until exhaustion. Energy efficiency was computed as the power output (watts converted in kJ/min) over exercise energy expenditure (in kJ/min) measured during the 1-hour submaximal bike test. To further define subject characteristics body composition was assessed using air displacement plethysmography and habitual physical activity was determined using an ActivPAL3 monitor.